

UCSF

UC San Francisco Previously Published Works

Title

Comparison of hepatocellular carcinoma conspicuity on hepatobiliary phase images with gadoxetate disodium vs. delayed phase images with extracellular cellular contrast agent

Permalink

<https://escholarship.org/uc/item/16s3j82b>

Journal

Abdominal Radiology, 41(8)

ISSN

2366-004X

Authors

Kim, So Yeon
Wu, En-Haw
Park, Seong Ho
[et al.](#)

Publication Date

2016-08-01

DOI

10.1007/s00261-016-0703-1

Peer reviewed



HHS Public Access

Author manuscript

Abdom Radiol (NY). Author manuscript; available in PMC 2017 February 08.

Published in final edited form as:

Abdom Radiol (NY). 2016 August ; 41(8): 1522–1531. doi:10.1007/s00261-016-0703-1.

Comparison of hepatocellular carcinoma conspicuity on hepatobiliary phase images with gadoxetate disodium vs. delayed phase images with extracellular cellular contrast agent

So Yeon Kim¹, En-Haw Wu², Seong Ho Park¹, Z. Jane Wang³, Thomas A. Hope³, Judy Yee³, Li-qin Zhao⁴, Wei-Chou Chang⁵, and Benjamin M. Yeh³

¹Department of Radiology and Research Institute of Radiology, Asan Medical Center, University of Ulsan College of Medicine, 388-1, Pungnap 2-dong, Songpa-ku, Seoul 138-736, Korea

²Department of Medical Imaging and Intervention, Chang Gung Memorial Hospital, Linkou and Chang Gung University College of Medicine, No. 5, Fuxing St, Guishan Township, Taoyuan, Taoyuan County 333, Taiwan

³Department of Radiology and Biomedical Imaging, University of California San Francisco, 505 Parnassus Ave, San Francisco, CA 94143-0628, USA

⁴Beijing Friendship Hospital, Capital Medical University, No 95, Yong'an Road, Xicheng District, Beijing 100050, China

⁵Tri-Service General Hospital and National Defense Medical Center, No.325, Sec. 2, Cheng-Kung Road, Neihu, Taipei, Taiwan

Abstract

Objective—To compare the conspicuity of hepatocellular carcinoma (HCC) on hepatobiliary phase of gadoxetate disodium-enhanced vs. delayed phase of gadodiamide-enhanced MR images, relative to liver function.

Methods and materials—We retrospectively identified 86 patients with newly diagnosed HCC between 2010 and 2013 and recorded the severity of liver disease by Child-Pugh class (CPC). 38 patients had gadodiamide-enhanced 5-min delayed and 48 had gadoxetate disodium-enhanced 20-

Correspondence to: Benjamin M. Yeh; ben.yeh@ucsf.edu.

Compliance with ethical standards

Human and animal rights statement All procedures performed in studies involving human participants were in accordance with the ethical standards of the institutional and/or national research committee and with the 1964 Helsinki declaration and its later amendments or comparable ethical standards. The requirement for informed consent was waived by our Institutional Review Board

Conflict of interest So Yeon Kim declares that she has no conflict of interest. En-Haw Wu declares that he has no conflict of interest. Seong Ho Park declares that he has no conflict of interest. Zhen Jane Wang received grants from the National Institutes of Health and is a shareholder of Nextrast, Inc. Thomas Hope is a consultant, grant recipient, and speaker for General Electric Healthcare. Judy Yee is a grant recipient of EchoPixel, Inc. and the National Institutes of Health. Li-qin Zhao declares that she has no conflict of interest. Wei-Chou Chang declares that he has no conflict of interest. Benjamin M. Yeh received grants from the National Institutes of Health, General Electric Healthcare, General Electric Global Research Center, and NeuWave Inc, received book royalties from Oxford University Press, and is a shareholder of Nextrast, Inc.

Ethical approval Our study was approved by our institutional review board and compliant with the Health Insurance Portability and Accountability Act.

Informed consent Informed consent was waived due to the retrospective nature of the study.

min delayed hepatobiliary MR images. The conspicuity of 86 HCCs (mean size, 2.7 cm) was graded visually on a 3-point scale and quantified by liver-to-tumor contrast ratios (LTC). The relative liver parenchymal enhancement (RPE) was measured. For different CPCs, we compared the conspicuity of HCC and RPE between gadodiamide and gadoxetate.

Results—In patients with CPC A, the visual conspicuity and LTC of the 27 HCCs imaged with gadodiamide were significantly lower than those of the 38 HCCs with gadoxetate ($P < 0.01$, < 0.01 , respectively). RPE was lower in gadodiamide scans than gadoxetate scans ($P < 0.01$). Conversely, in patients with CPC B and C, HCCs appeared more frequently as definite hypointensity when imaged with gadodiamide (72.7%, 8/11) than gadoxetate (20%, 2/10, $P = 0.03$). LTC (mean 18.1 vs. 7.5, $P = 0.04$) and RPE (mean 75.5 vs. 45.4, $P = 0.04$) was significantly higher in the gadodiamide than gadoxetate scans.

Conclusion—In patients with compromised liver function, hypointensity of HCC is more conspicuous in the gadodiamide delayed phase than the gadoxetate hepatobiliary phase. This likely reflects the high extracellular accumulation of gadodiamide and poor hepatocyte uptake of gadoxetate in patients with compromised liver function.

Keywords

Hepatocellular carcinoma; Gadoxetate; Washout; Liver MRI

For the diagnosis of hepatocellular carcinoma (HCC), contrast-enhanced computed tomography (CT) and magnetic resonance (MR) imaging are vital for tumor detection and diagnosis [1–3]. “Washout,” which refers to tumor hypointensity relative to liver parenchyma in the portal venous or delayed phase using conventional extracellular contrast material, is a key diagnostic feature of HCC in many guidance documents [1–3]. Recent studies on extracellular contrast agents report that washout is better seen in the delayed phase than in the portal venous phase, with 19–64% of HCCs exhibiting washout only on the delayed phase images after contrast injection [4, 5].

Gadoxetate disodium-enhanced MR imaging is a recent valuable addition to imaging work-up for HCC due to the advantage of hepatobiliary phase images [6, 7]. The primary advantage of hepatobiliary phase images is attributed to its potential for strong enhancement of hepatic parenchyma, which allows hypointense tumors to be seen with high conspicuity against the hyperintense liver parenchyma [8–13]. On gadoxetate-enhanced MR images, hypointensity of a lesion in the hepatobiliary phase is an important sign to differentiate HCC from arterially enhancing pseudolesions [8, 9]. Unfortunately, the hepatic parenchymal enhancement of gadoxetate-enhanced MR imaging may be diminished in patients with poor hepatic function [14–17], and this poor enhancement may reduce the visibility of HCC during the hepatobiliary phase in such patients [18, 19].

Recent work demonstrated that the hepatic parenchymal enhancement from extracellular CT contrast at delayed (equilibrium) phase imaging is more pronounced in patients with diffuse liver disease such as liver cirrhosis [20, 21]. This observation reflects the increased volume of hepatic extracellular space that is seen in diffuse liver disease and fibrosis. The increased volume of hepatic extracellular space results in proportionally greater amounts of

extracellular contrast material in the liver parenchyma at the delayed (equilibrium) phase of enhancement [20–23]. Unfortunately, the possibility that increased extracellular contrast material in diseased livers could result in an increased conspicuity of HCC at delayed phase MR images has not been studied in published reports. Furthermore, given the nonlinear relationship between signal intensity and contrast concentration on MR imaging [24], the applicability of this concept to clinical observation to MR imaging needs to be tested.

In addition, there is a paucity of publications that directly compare the diagnostic performance between gadoxetate and extracellular MR contrast agents [25, 26]. Importantly, prior comparisons of gadoxetate to extracellular MR contrast agents did not account for the severity of liver disease [25, 26].

Thus, the purpose of our study was to compare the conspicuity of HCC on hepatobiliary phase of gadoxetate disodium-enhanced vs. delayed phase of extracellular contrast (gadodiamide)-enhanced MR images relative to liver function.

Materials and methods

Our study was approved by our institutional review board and compliant with the Health Insurance Portability and Accountability Act. Informed consent was waived by our Institutional Review Board due to the retrospective nature of the study.

Study subjects

We searched the electronic database of our institution and identified 742 consecutive patients who underwent 1130 abdominal MR examinations obtained between January 2010 and June 2013. Among them, we retrospectively identified 102 patients (101 men & 1 woman; mean age, 63 years; range 49–81 years) with MR exams suggesting a newly developed HCC. Since our hospital is a military institution, our patients are skewed toward male gender. Of our initial patients, we excluded ten patients for the following reasons which may preclude the quantitative and visual assessment of signal intensity of the hepatic parenchyma or HCC: (1) infiltrative HCC ($n = 3$); (2) bile duct obstruction ($n = 1$); (3) more than 10 HCCs ($n = 3$); and (4) hyperintense HCCs on hepatobiliary phase images ($n = 3$). Of the remaining 92 patients, we further excluded three patients who did not have available relevant laboratory tests for the determination of liver disease severity within three months before or after liver MR examinations. In addition, we excluded three patients in whom HCCs were not confirmed by pathology or were not consistent with our reference standard (described below in detail). Thus, our study population consisted of 86 patients (86 men; mean age, 63 years; range 49–81 years) with HCCs.

Of the 86 patients, 51 patients had a single HCC and 30 patients had multiple HCCs (range of the number of HCC: 2–9). For the 30 patients with multiple HCCs, only the largest lesion in each patient was included for analysis to avoid clustering effects. Therefore, 86 HCCs in 86 patients were included in the analysis. The size of the 86 HCCs ranged from 1.0 to 9.1 cm (mean size \pm standard deviation, SD 2.7 ± 1.5 cm). One of the authors (9 years of experience in abdominal radiology), who was not involved in the subsequent image analysis, made a list indicating the size and locations of the target HCCs to be analyzed.

The diagnosis of HCC was confirmed pathologically for 29 lesions (24 lesions by surgery and 5 lesions by percutaneous biopsy). The remaining 57 HCC lesions were diagnosed according to the Liver Imaging Reporting and Data System (LI-RADS) version 2013.1 proposed by the American College of Radiology [27]. LI-RADS Category 4 or 5 lesions were classified as HCCs in this study. The 46 of the 57 lesions were reconfirmed by tumor recurrence or metastasis after local treatment ($n = 19$), interval growth ($n = 17$) at least 50% in diameter of the nodule within 6 months or 100% within 12 months in follow-up CT ($n = 2$) or MR ($n = 16$), lipidol uptake after transarterial chemoembolization ($n = 5$), and CT scans within one month of MR consistent with diagnostic criteria proposed by the American Association for the Study of Liver Diseases ($n = 5$) [3].

Patient characteristics

One of the authors (9 years of experience in abdominal imaging) who was not involved in imaging analysis for HCC, reviewed the electronic medical records and recorded clinical and laboratory data within 3 months before or after MR examinations (mean 13.2 days; range 0–69 days). These included age, gender, body weight (kg), total bilirubin (mg/dL), albumin (g/dL), international normalized ratio of prothrombin time (PT), creatinine (mg/dL) and estimated glomerular filtration rate (eGFR, mL/min/1.73 m²), the amount of ascites, and a history of hepatic encephalopathy. Using the clinical and laboratory data, the Child-Pugh class (CPC) [28] and the Model for End-Stage Liver Disease (MELD) score [29] was recorded.

MR imaging techniques

During the study period, two different MR contrast agents, gadoxetate disodium (Eovist; Bayer Healthcare, Wayne, NJ) and gadodiamide (Omniscan; GE Healthcare Medical Diagnostics, Little Chalfont, Buckinghamshire, UK) were used for liver MR examinations. To avoid biases related to repeat examinations, only the earliest MR examinations with the HCC diagnosis were included for analysis. Thus, the analysis included 48 MR scans obtained with gadoxetate disodium, and 38 scans with gadodiamide. Gadoxetate disodium was administered at a fixed dose of 10 mL per patient and gadodiamide was also administered at a fixed dose of 20 mL per patient. In previously published studies and current clinical practice, off-label fixed 10 mL doses of gadoxetate disodium are commonly used in order to increase arterial enhancement and improve lesion-to-liver contrast [13, 30–33]. In our institution, off-label use of gadodiamide was used during the study period to potentially increase the amount of gadolinium contrast agent for better vascular enhancement [34]. Gadoxetate was power injected at a rate of 1 mL/s and gadodiamide was power injected at a rate of 2 mL/s. Gadoxetate or gadodiamide injection was followed by 25 mL of saline flush at the same rate as the contrast administration.

Each patient underwent MR imaging on a 1.5-T magnetic resonance (MR) system (Magnetom Avanto; Siemens Medical Solutions, Erlangen, Germany) with a dedicated 6-channel torso array coil. Imaging protocols for both gadoxetate and gadodiamide groups included nonenhanced MR sequences and contrast-enhanced T1-weighted imaging. For both contrast agents, axial T1-weighted images were acquired in the arterial phase (determined using a fluoroscopic triggering method), venous phase (15 s after completion of arterial

phase images), and delayed phase (5 min following contrast injection) using a fat-suppressed, three-dimensional, spoiled gradient echo sequence (volumetric interpolated breath-hold examination, VIBE; Siemens) with the following scan parameters: TR/TE of 3.8 ms/1.7 ms; flip angle of 12°; field of view of 370 × 300 mm; matrix of 256 × 166; slice thickness of 3 mm; parallel imaging technique (GRAPPA; Siemens Medical Solutions) with an acceleration factor of two. For MR scans with gadoxetate, hepatobiliary phase images were obtained at 20 min after contrast administration with the same pulse sequence.

MR image analysis

Two abdominal radiologists (with 6 and 10 years of experience in abdominal imaging, respectively) evaluated MR images on the arterial, portal, and hepatobiliary phase images of the gadoxetate group and the arterial, portal, and delayed phase images of the gadodiamide group in consensus. During image interpretation, the readers referred to the list indicating the anatomic location and size of the target HCCs in order to identify the lesions correctly. While the readers were blinded to clinical data, they were not blinded to the MR contrast agent used, since delayed phase images of gadodiamide-enhanced MR and hepatobiliary phase images of gadoxetate-enhanced MR imaging are easily discernible.

The readers performed qualitative assessment of the conspicuity of HCCs. For this analysis, they visually compared the predominant signal intensity (SI) of HCCs to the SI of the surrounding hepatic parenchyma on hepatobiliary phase images for the gadoxetate group and delayed phase images for the gadodiamide group. The visual conspicuity for hypointensity of HCC was rated on a three-point scale (1, invisible; 2, fair; 3, excellent): grade 1, when the hypointensity of a lesion was invisible or barely depicted; grade 3, when a lesion was definitely hypointense compared to hepatic parenchyma. Grade 2 was applied to a lesion slightly hypointense which was not classified as grade 1 or grade 3.

Quantitative analysis of tumor conspicuity and hepatic parenchymal enhancement was performed on a commercially available workstation (Syngo, Siemens Medical Solutions, Erlangen, Germany). The readers placed region of interest (ROI) on the target HCC lesions and the nontumorous liver parenchyma, and measured the signal intensity on nonenhanced images, hepatobiliary phase images of gadoxetate-enhanced MR, and delayed phase images of gadodiamide-enhanced MR. ROIs of HCCs were drawn as large as possible excluding approximately 1 mm peripheral margin of the lesion in order to prevent partial volume averaging effect. The mean SI values for the HCC measured on two consecutive slices were used for analysis. The SI of the liver was obtained by averaging the SI values of three 1.5-cm-diameter circular ROIs which were positioned in areas devoid of large vessels, focal hepatic lesions, or prominent artifact. The standard deviation of the background noise was measured in the largest possible rectangular ROI placed in the phase-encoding direction outside the abdominal wall on nonenhanced and contrast-enhanced images. Liver-to-tumor contrast noise ratios (LTC) were calculated as follows for hepatobiliary phase image of gadoxetate-enhanced MR scans and delayed phase images of gadodiamide-enhanced MR: $[(SI_{LE} - SI_{TE})/SI_N]$, where SI_{LE} is the SI of the liver on enhanced images, SI_{TE} is the SI of the tumor on enhanced images, and SI_N is the SI of the background noise. The relative hepatic parenchymal enhancement (RPE) was calculated as follows: $(SNR_E - SNR_{NE})/$

$SNR_{NE} \times 100\%$, where SNR_E refers liver signal-to-noise ratio (SNR) in enhanced images and SNR_{NE} is unenhanced liver SNR. The SNR of the liver was calculated as the SI of the liver/SD of background noise. RPE served as a quantitative index of the relative SI increase of hepatic parenchyma at hepatobiliary phase images or delayed phase images compared to that of nonenhanced images.

Statistical analysis

Patient demographics, including age, body weight, eGFR, the CPC, and the size and location of HCCs, were compared between gadoxetate disodium-enhanced and gadodiamide-enhanced MR scans. Patients were then sub-divided into two groups based on the CPC: patients with normal liver function (CPC A) vs. patients with compromised liver function (CPC B & C). Subgroup analysis according to liver function was performed to compare the clinical and tumor characteristics between the two contrast agents. The numbers and the percentages of typical HCC on imaging in both groups as determined by the AASLD guidelines [3] the European Association for the Study of the Liver (EASL) criteria were also assessed [35].

We compared HCC conspicuity in terms of the conspicuity scores by visual assessment and LTC between the two contrast agents. Visual conspicuity scores as well as their distribution between the two contrast agents were compared. Hepatic parenchymal enhancement was evaluated by RPE. Subgroup analysis according to liver function was also done for the comparison for HCC conspicuity and hepatic parenchymal enhancement. The Spearman correlation coefficient (ρ) was used to examine the correlation between LTC or RPE and MELD score.

Statistical comparisons were performed using the Fisher's exact test for categorical variables and the independent *t* test or Mann–Whitney *U* test for quantitative variables. Statistical analyses were performed in SPSS (version 19, IBM). $P < 0.05$ was considered statistically significant.

Results

Patients demographics and HCC characteristics

Table 1 summarizes the patient demographics and HCC characteristics in both contrast groups. None of the tested variables was significantly different between the two groups. In the gadoxetate group, 38 (38/48, 79.2%) HCCs were found in patients with normal liver function and 10 (10/48, 20.8%; seven with CPC B and three with CPC C) HCCs were in patients with compromised liver function. The gadodiamide population was composed of 27 (27/38, 71.1%) HCCs in patients with normal liver function and 11 (11/38, 28.9%; nine with CPC B and two with CPC C) HCCs with compromised liver function. Due to the limited number of patients with compromised liver function, the patients with both CPC B and C were combined into a “compromised liver function” group. The distribution of patients according to liver function was not different between the two contrast groups ($P = 0.14$). In subgroup analyses, grouped by liver function, none of the patient demographics and HCC

characteristics were significantly different between the Child-Pugh A vs. the B and C groups (Table 1).

According to the EASL/AASLD criteria, 33 cases (33/48, 68.8%) were diagnosed as HCC in the gadoxetate disodium group, and 29 cases (29/38, 73.3%) were diagnosed as HCC in the gadodiamide group. In the gadoxetate disodium group, seven cases did not have arterial hypervascularity and eight cases did not show washout during the portal phase. In the gadodiamide group, five cases did not show arterial hypervascularity and four cases were not accompanied with washout during the portal or delayed phase images.

HCC conspicuity

When HCC conspicuity was compared without consideration of hepatic function (Table 2), the visual scores of HCC conspicuity on the hepatobiliary phase of gadoxetate disodium tended to be better than on the delayed phase of gadodiamide, but not significantly so ($P=0.12$). LTC was significantly higher in the gadoxetate than in the gadodiamide group ($P<0.01$).

In patients with normal hepatic function (Table 2), both visual conspicuity of HCCs and LTC were higher on the hepatobiliary phase of the gadoxetate-enhanced images than on the delayed phase of the gadodiamide-enhanced images ($P<0.01$, <0.01 , respectively). The opposite result was seen in patients with compromised liver function (Table 2): LTC was significantly lower in the gadoxetate group (mean LTC, 7.5) than in the gadodiamide group (mean LTC, 18.1) ($P=0.04$). The visual conspicuity scores in the gadoxetate group (mean 2) tended to be lower than that in the gadodiamide group (mean 2.5), but not significantly so ($P=0.10$). Figure 1 shows the distribution of the HCC conspicuity scores on the hepatobiliary phase images of gadoxetate-enhanced MR exams and on delayed phase images of gadodiamide-enhanced MR exams according to liver function of the patients. The distribution of the visual conspicuity was significantly different between the two groups in the subgroup analysis. In the patients with normal liver function, HCC was seen more frequently as definite hypointensity in gadoxetate-enhanced MR scans than in gadodiamide-enhanced MR scans. In the patients with compromised liver function, however, only 20% (2/10) of HCC appeared as a definite hypointensity when imaged with gadoxetate, while 72.7% (8/11) of HCC looked as a definite hypointensity when imaged with gadodiamide (Figs. 2, 3). Among all the four patients (two with normal liver function and two with compromised liver function) in whom the HCCs were invisible on the hepatobiliary phase of the gadoxetate-enhanced images, one of them with normal hepatic function showed washout during the portal phase of gadoxetate-enhanced images while the other three did not.

LTC showed significant negative correlation with MELD scores ($\rho = -0.627$, $P < 0.01$) in the gadoxetate group and marginally positive correlation ($\rho = 0.319$, $P = 0.05$) in the gadodiamide group.

Relative parenchymal enhancement

When the total study population was considered, RPE tended to be higher in hepatobiliary phase images of gadoxetate-enhanced MR exams (mean \pm SD, 79.2 ± 45.1) than in delayed phase images of gadodiamide-enhanced MR exams (mean \pm SD, 62.1 ± 32.1) ($P=0.11$).

When patients with normal hepatic function were separately assessed, RPE in hepatobiliary phase images of gadoxetate-enhanced MR scans (mean \pm SD, 88.3 ± 45.6) was significantly higher than that in delayed phase images of gadodiamide-enhanced MR scans (mean \pm SD, 56.9 ± 30.5) ($P < 0.01$). In contrast, in patients with compromised liver function, RPE in the hepatobiliary phase of the gadoxetate population (mean \pm SD, 45.5 ± 21.7) was significantly lower than that in the delayed phase of the gadodiamide population (mean \pm SD, 75.5 ± 33.8) ($P = 0.04$). Figure 4 shows RPE on the hepatobiliary phase images of gadoxetate-enhanced MR exams and on delayed phase images of gadodiamide-enhanced MR exams according to liver function of the patients.

In the gadoxetate group, RPE was significantly correlated with MELD scores ($\rho = -0.472$, $P < 0.01$), while no significant correlation was noted in the gadodiamide group ($\rho = 0.285$, $P = 0.08$).

Discussion

We found that hepatic function plays a key role in the conspicuity of HCC hypointensity in hepatobiliary phase images of gadoxetate disodium and delayed phase images of extracellular contrast agent (gadodiamide) liver MR. Hepatobiliary phase images of gadoxetate-enhanced exams outperform delayed phase images of gadodiamide-enhanced MR in depicting hypointensity of HCC in patients with normal liver function (Child-Pugh A). However, the opposite is true in patients with compromised liver function (Child-Pugh B/C), with decreased HCC conspicuity on the hepatobiliary phase images of gadoxetate-enhanced MR.

Despite the recent great attention to gadoxetate vs. the traditional use of extracellular contrast agents for the work-up for HCC, there is a paucity of data that compare the imaging with these two types of MR contrast agents directly [25, 26]. When we did not sub-stratify patients by the degree of liver function, our study supports a recent study showing a trend toward better diagnostic performance of gadoxetate disodium than that of gadopentetate dimeglumine (Magnevist, Bayer Schering Pharma) [26]. However, these previous publications [25, 26] comparing the two contrast agents did not consider liver function of patients. Our results provide a direct comparison between gadoxetate and extracellular MR contrast agents for the late phase of enhancement. The reason we focused primarily on the hepatobiliary phase images of gadoxetate disodium and delayed phase images of gadodiamide liver MR was that these late phases are where critical “wash-out” is generally sought [4, 5, 8–13]. Nevertheless, it should be noted that hypointensity on hepatobiliary phase images cannot be considered equivalent to true washout as depicted on portal venous phase (using extracellular MR contrast agents or gadoxetate) or delayed phase images (with extracellular contrast agents). A recent study demonstrated that to include hypointensity on hepatobiliary phase images of gadoxetate-enhanced MR imaging as a criterion to make a diagnosis of HCC could decrease the specificity [36].

It is known that liver function has an important influence on the degree of hepatic parenchymal enhancement and consequently HCC conspicuity on gadoxetate-enhanced MR scans [18, 19]. Our results are in agreement with those from prior studies, and additionally

showed that hepatic parenchyma enhancement as well as the HCC conspicuity on delayed phase images of extracellular contrast-enhanced MR exams can also be affected by liver function. Recent work using extracellular CT contrast demonstrated that the increased enhancement in delayed phase images is linearly related to the amount of liver fibrosis and correlates with the MELD scores [20, 21]. The increased liver enhancement at delayed phase imaging of extracellular contrast agent was attributed to the increased amount of extracellular contrast material that equilibrates into the expanded extracellular space secondary to liver fibrosis, edema, or inflammation [20–23]. This increased hepatic parenchymal enhancement, in turn, can explain the higher conspicuity of HCC in this group. The same phenomenon likely explains our finding of higher liver parenchymal enhancement observed with gadodiamide in patients with compromised liver function (CPC B/C). However, when we evaluated the correlation of LTC and RPE with MELD scores in the gadodiamide group, it did not show significant correlation possibly due to the nonlinear relationship between signal intensity and contrast concentration at MR imaging [24]. Further studies are warranted to prove the relationship between liver parenchymal enhancement on extracellular contrast agent-enhanced MR and liver functional parameters.

Our study found that the primary diagnostic advantage of gadoxetate disodium-enhanced MR from strong hepatic enhancement and high lesion conspicuity on hepatobiliary phase images can be maximized in patients with normal liver function [8–13]. However, in patients with compromised liver function, extracellular contrast may be more appropriate for detecting HCC because of the increased hepatic parenchymal enhancement at delayed imaging in these patients. The results of our study suggest the importance of considering liver function when selecting MR contrast agents for liver MR imaging. In addition, an optimized protocol including high flip angles [37] for the hepatobiliary phase could be considered to improve liver-to-lesion contrast in patients with compromised liver function.

Our study has several limitations. First, only 34% HCCs in our study were confirmed by histopathology. Therefore, we did not have information on the histologic and molecular features of HCCs, which may affect lesion conspicuity [38]. However, it is virtually impossible or even unethical to obtain histopathologic diagnosis of all HCCs, as imaging criteria is widely accepted to make the diagnosis of HCC in the majority of patients [1–3]. In addition, the LI-RADS criteria were used to make image-based diagnosis of HCC in our study. Since the diagnostic performance of LI-RADS criteria has not been completely proven yet, we reconfirmed the diagnosis of HCCs with other additional methods when possible. Second, our study included a limited number of patients, particularly those with compromised liver function. The limited number of patients in the group of compromised liver function prevented separate analysis of Child-Pugh B vs. C. Third, we did not assess the diagnostic performance of HCC using the other available MR sequences, although hypointensity on delayed or hepatobiliary phase images evaluated in our study is a key diagnostic feature of HCC. Future studies are warranted to compare the diagnostic performance of HCC using other MR sequences including arterial phase images between gadoxetate-enhanced and extracellular contrast-enhanced MR exams. Fourth, we administered off-label fixed doses of gadoxetate disodium and gadodiamide instead of weight-adjusted approved doses. It can be a possible confounder of our results. Fifth, owing to spatially variable noise distribution, measurement of SNR may not be reliable on MR

images obtained with parallel imaging techniques [39]. However, we put ROIs at the same locations of the liver when we measured SNR in different phases of images and we used ratios of SNR rather than SNR itself. Thus, the effect of spatially variable noise distribution may be minimized. Lastly, our study group had a skewed age and gender distribution and consisted of mostly of elderly men because it was performed in a military hospital. Although our study results may not be readily generalized, they do provide impetus for a direct comparison between gadoxetic acid and gadodiamide MR for HCC diagnosis in patients with compromised liver function.

In conclusion, in patients with compromised liver function, hypointensity of HCC is more conspicuous on the delayed phase with gadodiamide than on the hepatobiliary phase with gadoxetate disodium. This likely reflects increased gadodiamide accumulation in the expanded extracellular space and poor hepatocyte uptake of gadoxetate in patients with compromised liver function. Consideration of liver function may be valuable when choosing between hepatobiliary and extracellular contrast material for the imaging of possible HCC.

References

1. Bruix J, Sherman M, Llovet JM, et al. Clinical management of hepatocellular carcinoma. Conclusions of the Barcelona-2000 EASL conference. European Association for the Study of the Liver. *J Hepatol.* 2001; 35:421–430. [PubMed: 11592607]
2. Omata M, Lesmana LA, Tateishi R, et al. Asian Pacific Association for the Study of the Liver consensus recommendations on hepatocellular carcinoma. *Hepatol Int.* 2010; 4:439–474. [PubMed: 20827404]
3. Bruix J, Sherman M. American Association for the Study of Liver D. Management of hepatocellular carcinoma: an update. *Hepatology.* 2011; 53:1020–1022. [PubMed: 21374666]
4. Jang HJ, Kim TK, Khalili K, et al. Characterization of 1-to 2-cm liver nodules detected on HCC surveillance ultrasound according to the criteria of the American Association for the Study of Liver Disease: is quadriphasic CT necessary? *AJR Am J Roentgenol.* 2013; 201:314–321. [PubMed: 23883211]
5. Luca A, Caruso S, Milazzo M, et al. Multidetector-row computed tomography (MDCT) for the diagnosis of hepatocellular carcinoma in cirrhotic candidates for liver transplantation: prevalence of radiological vascular patterns and histological correlation with liver explants. *Eur Radiol.* 2010; 20:898–907. [PubMed: 19802612]
6. Kudo M. Will Gd-EOB-MRI change the diagnostic algorithm in hepatocellular carcinoma? *Oncology.* 2010; 78(Suppl 1):87–93.
7. Fowler KJ, Brown JJ, Narra VR. Magnetic resonance imaging of focal liver lesions: approach to imaging diagnosis. *Hepatology.* 2011; 54:2227–2237. [PubMed: 21932400]
8. Motosugi U, Ichikawa T, Sou H, et al. Distinguishing hypervascular pseudolesions of the liver from hypervascular hepatocellular carcinomas with gadoxetic acid-enhanced MR imaging. *Radiology.* 2010; 256:151–158. [PubMed: 20574092]
9. Sun HY, Lee JM, Shin CI, et al. Gadoxetic acid-enhanced magnetic resonance imaging for differentiating small hepatocellular carcinomas (< or =2 cm in diameter) from arterial enhancing pseudolesions: special emphasis on hepatobiliary phase imaging. *Invest Radiol.* 2010; 45:96–103. [PubMed: 20057319]
10. Ahn SS, Kim MJ, Lim JS, et al. Added value of gadoxetic acid-enhanced hepatobiliary phase MR imaging in the diagnosis of hepatocellular carcinoma. *Radiology.* 2010; 255:459–466. [PubMed: 20413759]
11. Chou CT, Chen YL, Su WW, et al. Characterization of cirrhotic nodules with gadoxetic acid-enhanced magnetic resonance imaging: the efficacy of hepatocyte-phase imaging. *J Magn Reson Imaging.* 2010; 32:895–902. [PubMed: 20882620]

12. Yu MH, Kim JH, Yoon JH, et al. Small (< 1-cm) hepatocellular carcinoma: diagnostic performance and imaging features at gadoxetic acid-enhanced MR imaging. *Radiology*. 2014; 271:748–760. [PubMed: 24588677]
13. Bashir MR, Gupta RT, Davenport MS, et al. Hepatocellular carcinoma in a North American population: does hepatobiliary MR imaging with Gd-EOB-DTPA improve sensitivity and confidence for diagnosis? *J Magn Reson Imaging*. 2013; 37:398–406. [PubMed: 23011874]
14. Bae KE, Kim SY, Lee SS, et al. Assessment of hepatic function with Gd-EOB-DTPA-enhanced hepatic MRI. *Dig Dis*. 2012; 30:617–622. [PubMed: 23258104]
15. Motosugi U, Ichikawa T, Oguri M, et al. Staging liver fibrosis by using liver-enhancement ratio of gadoxetic acid-enhanced MR imaging: comparison with aspartate aminotransferase-to-platelet ratio index. *Magn Reson Imaging*. 2011; 29:1047–1052. [PubMed: 21775085]
16. Yamada A, Hara T, Li F, et al. Quantitative evaluation of liver function with use of gadoxetate disodium-enhanced MR imaging. *Radiology*. 2011; 260:727–733. [PubMed: 21712472]
17. Kim HY, Choi JY, Park CH, et al. Clinical factors predictive of insufficient liver enhancement on the hepatocyte-phase of Gd-EOB-DTPA-enhanced magnetic resonance imaging in patients with liver cirrhosis. *J Gastroenterol*. 2013; 48:1180–1187. [PubMed: 23354621]
18. Kim JY, Lee SS, Byun JH, et al. Biologic factors affecting HCC conspicuity in hepatobiliary phase imaging with liver-specific contrast agents. *AJR Am J Roentgenol*. 2013; 201:322–331. [PubMed: 23883212]
19. Kim AY, Kim YK, Lee MW, et al. Detection of hepatocellular carcinoma in gadoxetic acid-enhanced MRI and diffusion-weighted MRI with respect to the severity of liver cirrhosis. *Acta Radiol*. 2012; 53:830–838. [PubMed: 22847903]
20. Varenika V, Fu Y, Maher JJ, et al. Hepatic fibrosis: evaluation with semiquantitative contrast-enhanced CT. *Radiology*. 2013; 266:151–158. [PubMed: 23169796]
21. Zissen MH, Wang ZJ, Yee J, et al. Contrast-enhanced CT quantification of the hepatic fractional extracellular space: correlation with diffuse liver disease severity. *AJR Am J Roentgenol*. 2013; 201:1204–1210. [PubMed: 24261358]
22. Aime S, Caravan P. Biodistribution of gadolinium-based contrast agents, including gadolinium deposition. *J Magn Reson Imaging*. 2009; 30:1259–1267. [PubMed: 19938038]
23. Faria SC, Ganesan K, Mwangi I, et al. MR imaging of liver fibrosis: current state of the art. *Radiographics*. 2009; 29:1615–1635. [PubMed: 19959511]
24. Materne R, Smith AM, Peeters F, et al. Assessment of hepatic perfusion parameters with dynamic MRI. *Magn Reson Med*. 2002; 47:135–142. [PubMed: 11754452]
25. Vogl TJ, Kummel S, Hammerstingl R, et al. Liver tumors: comparison of MR imaging with Gd-EOB-DTPA and Gd-DTPA. *Radiology*. 1996; 200:59–67. [PubMed: 8657946]
26. Park G, Kim YK, Kim CS, et al. Diagnostic efficacy of gadoxetic acid-enhanced MRI in the detection of hepatocellular carcinomas: comparison with gadopentetate dimeglumine. *Br J Radiol*. 2010; 83:1010–1016. [PubMed: 20682591]
27. The American College of Radiology. [Accessed April, 2014] Liver Imaging Reporting and Data System (LI-RADS) version 2013.1. 2013. <http://www.acr.org/Quality-Safety/Resources/LIRADS/>
28. Pugh RN, Murray-Lyon IM, Dawson JL, et al. Transection of the oesophagus for bleeding oesophageal varices. *Br J Surg*. 1973; 60:646–649. [PubMed: 4541913]
29. Tschirch FT, Struwe A, Petrowsky H, et al. Contrast-enhanced MR cholangiography with Gd-EOB-DTPA in patients with liver cirrhosis: visualization of the biliary ducts in comparison with patients with normal liver parenchyma. *Eur Radiol*. 2008; 18:1577–1586. [PubMed: 18369632]
30. Motosugi U, Ichikawa T, Sano K, et al. Double-dose gadoxetic acid-enhanced magnetic resonance imaging in patients with chronic liver disease. *Invest Radiol*. 2011; 46:141–145. [PubMed: 21139506]
31. Davenport MS, Viglianti BL, Al-Hawary MM, et al. Comparison of acute transient dyspnea after intravenous administration of gadoxetate disodium and gadobenate dimeglumine: effect on arterial phase image quality. *Radiology*. 2013; 266:452–461. [PubMed: 23192781]
32. Davenport MS, Caoili EM, Kaza RK, Hussain HK. Matched within-patient cohort study of transient arterial phase respiratory motion-related artifact in MR imaging of the liver: gadoxetate disodium versus gadobenate dimeglumine. *Radiology*. 2014; 272:123–131. [PubMed: 24617733]

33. Pietryga JA, Burke LM, Marin D, et al. Respiratory motion artifact affecting hepatic arterial phase imaging with gadoxetate disodium: examination recovery with a multiple arterial phase acquisition. *Radiology*. 2014; 271:426–434. [PubMed: 24475864]
34. Kittner T, Rudolf J, Fages JF, et al. Efficacy and safety of gadodiamide (Gd-DTPA-BMA) in renal 3D-magnetic resonance angiography (MRA): a phase II study. *Eur J Radiol*. 2007; 64:456–464. [PubMed: 17412546]
35. European Association for the Study of the Liver, European Organisation for Research and Treatment of Cancer. EASL-EORTC clinical practice guidelines: management of hepatocellular carcinoma. *J Hepatol*. 2012; 56:908–943. [PubMed: 22424438]
36. Joo I, Lee JM, Lee DH, et al. Noninvasive diagnosis of hepatocellular carcinoma on gadoxetic acid-enhanced MRI: can hypointensity on the hepatobiliary phase be used as an alternative to washout? *Eur Radiol*. 2015; 25:2859–2868. [PubMed: 25773941]
37. Bashir MR, Husarik DB, Ziemlewicz TJ, et al. Liver MRI in the hepatocyte phase with gadolinium-EOB-DTPA: does increasing the flip angle improve conspicuity and detection rate of hypointense lesions? *J Magn Reson Imaging*. 2012; 35:611–616. [PubMed: 22034383]
38. Kitao A, Zen Y, Matsui O, et al. Hepatocellular carcinoma: signal intensity at gadoxetic acid-enhanced MR imaging-correlation with molecular transporters and histopathologic features. *Radiology*. 2010; 256:817–826. [PubMed: 20663969]
39. Dietrich O, Raya JG, Reeder SB, et al. Measurement of signal-to-noise ratios in MR images: influence of multichannel coils, parallel imaging, and reconstruction filters. *J Magn Reson Imaging*. 2007; 26:375–385. [PubMed: 17622966]

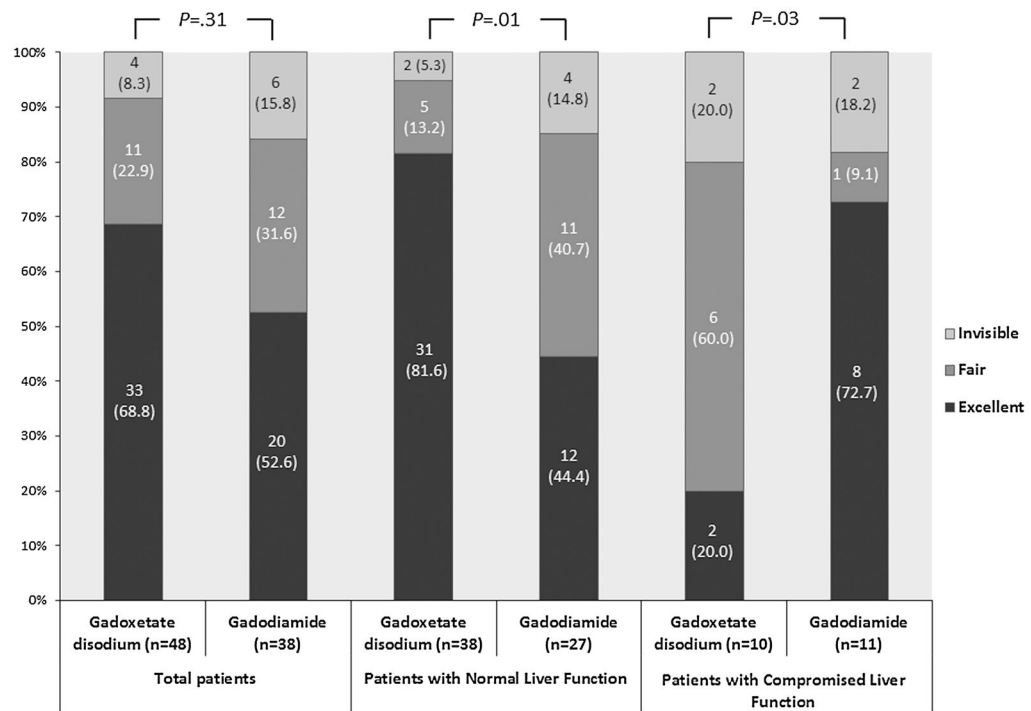


Fig. 1. Comparison of visual conspicuity of HCC between hepatobiliary phase images of gadoxetate and delayed phase images of gadodiamide relative to liver function of patients. The numbers in the bars indicate the number of the patients in each category, with the percentages in parentheses. The P values are from comparisons of the distribution of visual conspicuity scores between the two contrast agents.

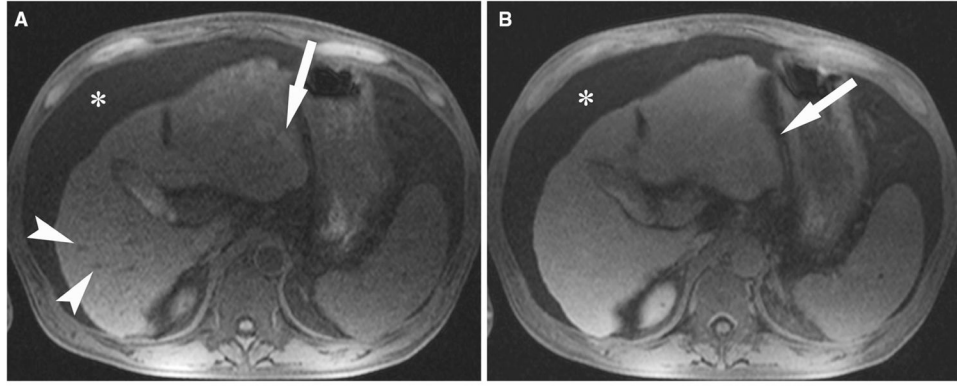


Fig. 2. Gadoxetate-enhanced MR in a 60-year-old male patient with CPC C. **A** The nonenhanced image reveals a HCC (*arrow*) located in left lobe of the liver. The HCC (*arrow*) appears isointense. Note that the portal veins (*arrowheads* in **A**) are not identified on the hepatobiliary phase image, which probably indicates insufficient enhancement of the hepatic parenchyma. Large ascites (*asterisks*) is also seen. **B** On the hepatobiliary phase image, the HCC (*arrow*) looks isointense compared to the surrounding hepatic parenchyma. LTC was measured as 2.6 and RPE was 27.3.

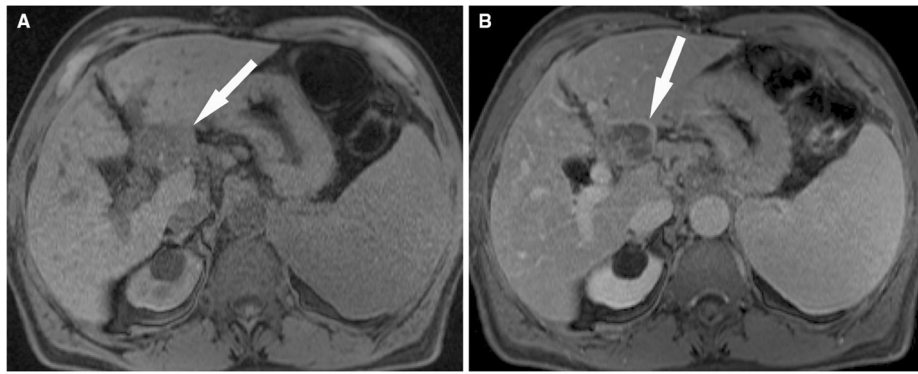


Fig. 3. Gadolinium-enhanced MR in a 65-year-old male with CPC C. **A** HCC (*arrow*) located in left lobe of the liver is seen as a subtle hypointense mass on the nonenhanced image. **B** On the delayed phase image, the HCC (*arrow*) appears as a definite hypointense mass with in comparison to the hepatic parenchyma. LTC was measured as 44.7 and RPE was 53.

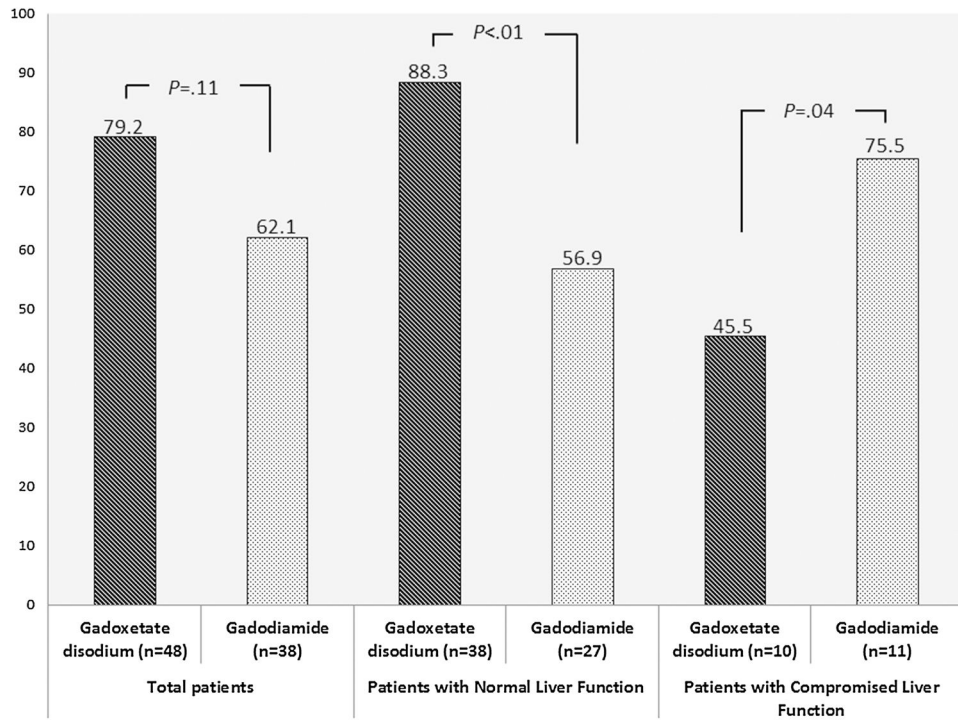


Fig. 4. Comparison of relative parenchymal enhancement between hepatobiliary phase images of gadoxetate and delayed phase images of gadodiamide relative to liver function of patients. The numbers above the bars indicate the mean value of relative parenchymal enhancement in each category. The *P* values are from comparisons of relative parenchymal enhancement between the two contrast agents.

Demographic Data of Study Population and HCC Characteristics

Table 1

Characteristics	All patients (n = 48)		Patients with Normal Liver Function (n = 38)		Patients with Compromised Liver Function (n = 10)	
	Gadoxetate disodium (n = 48)	Gadodiamide (n = 38)	Gadoxetate disodium (n = 38)	Gadodiamide (n = 27)	Gadoxetate disodium (n = 10)	Gadodiamide (n = 11)
Age (years)	63.0 ± 7.6	63.2 ± 6.8	64.2 ± 7.6	62.8 ± 5.9	58.2 ± 6.0	64.1 ± 8.9
Body weight (kg)	88.2 ± 17.6	85.5 ± 12.8	88.8 ± 17.9	88.4 ± 13.4	85.9 ± 17.0	78.6 ± 8.6
eGFR (mL/min/1.73 m ²)	97.4 ± 28.3	96.6 ± 30.9	97.3 ± 25.3	99.4 ± 25.5	97.4 ± 39.4	89.8 ± 42.1
Size of HCC (cm)	2.8 ± 1.6	2.5 ± 1.4	2.7 ± 1.5	2.5 ± 1.7	2.9 ± 2.0	2.4 ± 0.9
Location of HCC* (Rt lobe vs. Lt lobe)	32 (66.7) vs. 16 (33.3)	27 (71.1) vs. 11 (28.9)	28 (73.7) vs. 10 (26.3)	19 (70.4) vs. 8 (29.6)	4 (40.0) vs. 6 (60.0)	8 (72.7) vs. 3 (27.3)

Unless otherwise specified, data are mean ± standard deviation

eGFR, estimated glomerular filtration rate; Rt, right; Lt, left

* Data are the number of HCCs and data in parentheses are the percentages

Conspicuity of HCC

Table 2

Characteristics	All patients		Patients with normal liver function		Patients with compromised liver function				
	Gadoxetate disodium (n = 48)	Gadodiamide (n = 38)	P values	Gadoxetate disodium (n = 38)	Gadodiamide (n = 27)	P values	Gadoxetate disodium	Gadodiamide (n = 11)	P values
Visual scores	2.6 ± 0.4	2.3 ± 0.6	0.12	2.8 ± 0.3	2.3 ± 0.7	<0.01	2 ± 0.7	2.5 ± 0.7	0.10
LTC	25.6 ± 19.2	13.9 ± 12.8	<0.01	30.4 ± 18.7	12.2 ± 12.5	<0.01	7.5 ± 5.1	18.1 ± 13.3	0.04

Data are mean ± standard deviation in parentheses

LTC, liver-to-tumor contrast noise ratio